PCCP

Accepted Manuscript

ROYAL SOCIETY OF CHEMISTRY

www.rsc.org/pccp

Journal Name

ARTICLE

A new perspective on the process of intrinsic point defects in α-Al_2O_3

Received 00th January 20xx,
Accepted 00th January 20xx

DOI: 10.1039/x0xx00000x

www.rsc.org/

Xin Xiang,[a] Guikai Zhang, Xiaolin Wang*, Tao Tang, Yan Shi

First-principle plane-wave pseudopotential calculations have been performed to study the charge states and energetics of intrinsic point defects as vacancies, interstitials and antisite atoms in α-Al_2O_3, and thus a new perspective on the process of intrinsic point defects has been proposed. Considering the various charge states for each intrinsic point defects, V_{Al}^{3-}, V_O^{0}, Al_i^{3+}, O_i^{2-}, Al_O^{3+}, and O_{Al}^{3-}, not all in their fully ionized states are found to be most stable and in pure Al_2O_3. From the formation energies of individual point defects, the antisite atom O_{Al} will be readily formed in α-Al_2O_3 in an O-rich environment. By combination of charge states and formation energies, the defect types of Schottky, Al Frenkel and antisite pair formed are found to be dependent on the O condition, and the most stable Schottky defect type is not the common considered $\{3V_O^{2+}{:}2V_{Al}^{3-}\}$. There are two types of possible O Frenkel defect under both O conditions, yet the most stable defect is $\{O_i^{1+}{:}V_O^{1-}\}$ rather than the common believed $\{O_i^{2+}{:}V_O^{2-}\}$. The bizarre configuration and charge state of Schottky and Frenkel defects predicated in this work provides a new perspective on the process of intrinsic point defects in α-Al_2O_3.

1. Introduction

α-Al_2O_3, the most thermodynamically stable phase of alumina, is of great interest to industry such as catalyst supports, electronics substrates, optical device, oxidation and corrosion protective scales, thermal barrier coatings, and tritium permeation barriers in future fusion reactors [1-6]. However, both the bulk and surface properties (atomic transport, surface stability and activity, etc.) of α-Al_2O_3 are strongly dependent on the defect chemistry (defect type, charge state, configuration, formation energy, concentration, etc.), which will exert a significant influence on the final material performances and relevant functions [5-10]. Therefore, the knowledge of the defect chemistry in α-Al_2O_3 is essential in scientific and technologic interests.

Much effort has been devoted to the point defects in α-Al_2O_3, both from experimental [11-17] and theoretically [5-10, 18-25] aspects. In the last centenary, electrical and/or ionic conductivity [11, 12] measurements were commonly adopted to experimentally determine the defect structure in α-Al_2O_3, and creep [13] and optical spectrum [14] analysis methods were also utilized. However, these techniques encountered some difficulties that α-Al_2O_3 samples must be doped with donors or acceptors [12,13] (unintentionally doped also included [11]), and the experiments usually had to be conducted at rather high temperatures (over 1450°C) [11-13]. The reason is that Al_2O_3 is an insulator ceramics at low temperatures but a mixed conductor at high temperatures, and the electroconductivity depends also on oxygen pressure and doping species [12]. Therefore, advanced techniques such as high temperature positron annihilation spectroscopy [15, 16], thermally stimulated luminescence [16] and low temperature photoluminescence [17] were employed in recent years. These new techniques can only describe vacancy-type defects like alumina vacancy [15, 16], F- or F_2-type center (an isolated and two associated oxygen vacancies occupied by two and four electrons, respectively) [17], yet cannot give a whole picture of all types of point defects in α-Al_2O_3. Moreover, it is hard to obtain a perfect pure α-Al_2O_3 sample in experiment, and the unintentionally doped trace impurity, even with a concentration of an order of a few ppm, will dominate the defect chemistry in α-Al_2O_3 [18]. In any case, the point defect chemistry of α-Al_2O_3 must be clearly understood, since it is the foundation of exploring the fascinating material property of α-Al_2O_3.

Considering the difficulty and indirectness in the experimental defect identification for Al_2O_3, theoretical predicating and / or modeling have been employed and demonstrated usefulness in the area of the defect chemistry of Al_2O_3 [5-10, 18-25]. In earlier years, empirical and semiempirical methods such as molecular dynamic simulations based on potential functions [18-20] and shell-model calculations [21] were often used. Recently, thanks to the great progress achieved in supercomputers, first-principle calculations have emerged as a powerful tool for understanding point defects (neutral and/or charged) in Al_2O_3, which can be supportive and complementary for experimental findings [8]. As far as we know, four types of isolated point defects i.e. interstitials (Al_i, O_i) and vacancies (V_{Al}, V_O) in α-Al_2O_3 were mainly studied, and it is generally believed that intrinsic point defect in α-Al_2O_3 presents with their full formal charges: Al_i^{3+}, O_i^{2-}, V_{Al}^{3-} and V_O^{2+}

Institute of Materials, China Academy of Engineering Physics, 621907, Jiangyou, China. E-mail: xlwang@caep.cn; Fax: +86 81636 25900; Tel: +86 81636 26483.

[26]; while the other two point defects i.e. antisite atoms (O_{Al}, Al_O) were seldom involved. The most proposed reason is that antisite defects could not form easily for their high formation energy in metallic oxides [27, 28], but for α-Al_2O_3 convincible evidence is lacked. On the other hand, the defect processes (formation of Frenkel pair and Schottky defect) were mainly studied by empirical and semiempirical methods [18-21]. Controversy emerged between the results by empirical and semiempirical simulations as to which is dominant in Al_2O_3. Dienes et al.[21] showed that the formation of Schottky defects is energetically more favorable than that of Frenkel defects, while later calculations [18-20] showed that the oxygen Frenkel pair possess a lower formation energy than Schottky defects. The reason was attributed to the different potential parameters used for describing properties of Al_2O_3, which is not easy to verify whether the potential parameters are appropriate for defect simulations or not [19]. Moreover, the process of defect formation was assumed artificially by charge neutral combinations of anion- and cation-ions with their full formal charges [26], i.e. anion Frenkel (V_O^{2+}+O_i^{2-}), cation Frenkel (V_{Al}^{3-}+Al_i^{3+}), and Schottky defect ($2V_{Al}^{3-}$+$3V_O^{2+}$). As a matter of fact, the charge state of point defects in Al_2O_3 varies with oxygen potential and Fermi energy [29], and the equilibrium charge state for V_O is neutral, not +2 charged by the most recent first-principle study [6]. Therefore, much work still needs to be done to clarify the defect process in Al_2O_3.

In this work, the first-principle plane-wave pseudopotential method is used to investigate the formation energies and charge states of intrinsic point defects and their variations with oxygen potential in α-Al_2O_3. Based on these obtained results, a new perspective on the defect process in α-Al_2O_3 is proposed.

2. Computational method and model

The DMol3 [30] package in Materials Studio of Accelrys Inc was utilized to conduct all the first-principle calculations in this work. The exchange-correlation potential was treated in the Generalized Gradient Approximation (GGA), as parameterized in Perdew-Wang (PW91) [31]. The core treatment was done within the framework of all electron [32] and double numerical quality basis set with polarization functions (DNP) [33]. A convergence tolerance of energy of 1.0×10^{-5} Ha/atom, a maximum force of 2.0×10^{-3} Ha/Å, a maximum displacement of 5.0×10^{-3} Å, and a global orbital cutoff of 4.3 Å were used for all the calculations in the premise of spin unpolarization, giving energies computationally converging to within 2 meV/atom, which is sufficient to converge our results.

During geometry optimization, the periodic boundary condition was adopted, and the crystal lattice and atomic positions were fully relaxed. Using a 3×3×1 k-point mesh, the optimized crystal parameters (a=b=4.821 Å, c=13.105 Å, α=β=90°, γ=120°) of corundum structured α-Al_2O_3 agreed well with the experimental values (a=b=4.759 Å, c=12.991 Å) [34] and other theoretical results [29, 34]. The obtained band gap was 6.18 eV, 2.62 eV smaller than the experimental value of 8.80 eV [29, 34], for which the reason is often attributed to the common underestimation of band gap for metal oxides by the first-principle method [22, 29]. In a word, the parameters selected were sufficiently reasonable for the following calculations.

A 36-layer (2×2×2) α-Al_2O_3 supercell containing 144 O and 96 Al atoms was built for defect studies. After fully optimization with the crystal lattice and atomic positions, one isolated intrinsic point defect of vacancy (V_O, V_{Al}), interstitial (O_i, Al_i) and antisite atom (O_{Al}, Al_O) was created by removing, introducing and substituting a corresponding atom in the α-Al_2O_3 supercell, respectively, producing a defect concentration of ~0.4% in the bulk. Though it is still a relative bigger defect concentration than that under real material service condition, the isolated defect species was created in the nearby of geometry center of supercell in order to exclude possible defect self-interaction. However, defects in pure α-Al_2O_3 bulk can only exist in charge neutral combinations. Four typical defect processes of forming Schottky defect, cation Frenkel, anion Frenkel and antisite pair were considered. The Schottky defect is composed of several V_O and V_{Al} (mV_O+nV_{Al}), and the Frenkel pair incorporates a vacancy and corresponding interstitial atom (O_i+V_O, Al_i+V_{Al}). As for the antisite pair, it combines two types of antisite atoms (O_{Al} and Al_O) separated by different distances. During defect calculations, the crystal lattice was constrained, and all atoms except for those in the upper ten layers and the bottom ten layers of the supercell were fully relaxed. The Brillouin zone sampling was changed with a 2×2×1 k-point mesh.

The formation energy $\Delta E^f_{def}(X,q)$ of defect species X in charge state q is given by the following equation [29]:

$$\Delta E^f_{def}(X,q) = E^{tot}_{def} - E^{tot}_{perf} + \sum_i \Delta n_i \mu_i + qE_F$$

Where E^{tot}_{def} and E^{tot}_{perf} are the total energies of the defect and perfect supercells, respectively, Δn_i is the number of atom species i added (negative Δn_i) or removed (positive Δn_i) to create a defect, μ_i is the chemical potential of atom of element i (O or Al), and E_F is the Fermi energy within the gap of α-Al_2O_3.The chemical potentials of μ_{Al} and μ_O are not independent, but are constrained by the equilibrium condition of $2\mu_{Al}+3\mu_O=\mu_{Al2O3}$, where μ_{Al2O3} is the chemical potential of Al_2O_3 molecule. Moreover, the atomic chemical potentials are set by experimental conditions such as temperature, pressure and oxygen potential. Two extreme conditions of O-rich (Al-deficient) and O-deficient (Al-rich) are considered, since the working condition of Al_2O_3 is relative temperature and pressure fixed. For the O-rich condition, μ_O is determined to be half of the total energy of an O_2 molecule, i.e. $\mu_O=\mu_{O2}/2$, resulting in $\mu_{Al}=(\mu_{Al2O3}-3\mu_O)/2$. For the O-deficient condition, μ_{Al} is determined to be the total energy of Al unit cell, i.e. $\mu_{Al}=\mu_{Al}^{metal}$, yielding $\mu_O=(\mu_{Al2O3}-2\mu_{Al})/3$. The Fermi energy E_F varies from the top of valence band to the bottom of conduction band, i.e. lies in the range of 0 to E_g, where E_g is the band gap of perfect crystal. However, the GGA calculations often underestimate E_g with contrast to the experimental value, exerting an influence on the formation energies of intrinsic point defects in α-Al_2O_3 [35]. In this work, similar to other studies [6, 28], the formation energies were corrected by rigidly shifting the conduction band upward to match the experimental E_g of 8.8 eV. For each defect species, the charge state q varies from neutral to fully ionized states, i.e. 0~+2 for V_O, -3~0 for V_{Al}, -2~0 for O_i, 0~+3 for Al_i, -5~0 for O_{Al}, and 0~+5 for Al_O.

3. Results and discussion

3.1 Isolated intrinsic point defects in α-Al_2O_3

Fig.1 shows the formation energies of six types of isolated intrinsic point defects in various charge states in α-Al_2O_3 as a function of the Fermi level E_F. In this figure, results under the extreme conditions of O-rich (Fig.1a) and O-deficient (Fig.1b) are exhibited. Under the O-rich condition (Fig.1a), the most stable charge state for each defect species is dependent on the E_F position. When E_F is located near the top of valence band, the stable charge states for respective defect species are V_O^{2+}, Al_i^{3+}, V_{Al}^{0}, O_{Al}^{0}, Al_O^{5+} and O_i^{0} within the rising order of formation energies; and that will be O_{Al}^{5-}, V_{Al}^{3-}, O_i^{2-}, V_O^{0}, Al_i^{0} and Al_O^{0} when E_F is close to the bottom of conduction band. As for the insulating system of pure α-Al_2O_3, the equilibrium Fermi level E_F can be chose at the midpoint of E_g [36], i.e. 4.4 eV, labeled as dashed line in Fig.1. It can be seen that the most stable charge states of Al_i, O_i and V_{Al} are fully ionized at $E_g/2$, namely, Al_i^{3+}, O_i^{2-}, and V_{Al}^{3-}. As for V_O, the most stable charge state is neutral (V_O^{0}), for which two electrons remain at the position of O atom removed, that is F-center forms in α-Al_2O_3 as demonstrated by optical experiments [17, 37]. This finding of α-Al_2O_3 is different from earlier calculations [29], but is consistent with the most recently results [6, 22]. Therefore, it is easy to understand the most stable charge for Al_O is +3 at $E_g/2$, since Al_O forms via adding an Al atom to the existing O vacancy. On the other hand, the most stable charge state for O_{Al} is -3 at $E_g/2$, which may resulting from a neutral O atom located a -3 charged Al vacancy. That is because the main charge state of V_{Al} is -3, and the formation energy of V_{Al} is smallest around the Fermi energy. It is found that the relative stability of intrinsic point defects in α-Al_2O_3 under the O-rich condition is $V_{Al}^{3-} > O_{Al}^{3-} > O_i^{2-} > V_O^{0} > Al_i^{3+} > Al_O^{3+}$ at the Fermi energy.

The charge states and their variation tendencies of each defect species in α-Al_2O_3 with the Fermi level E_F under the O-deficient condition are the same as what under the O-rich condition within the range of 0~E_g, shown in Fig.1b. However, the relative stability of each intrinsic point defect has a remarkable change with E_F, compared with that under the condition of O-rich. For instance, the relative stability at the Fermi energy under the O-deficient condition is $V_{Al}^{3-}>V_O^{0}>O_i^{2-}>Al_i^{3+}>O_{Al}^{3-}>Al_O^{3+}$. On the other hand, the formation energy of respective defect at the same E_F position differs greatly under both O conditions. As for V_{Al}, the formation energy is -4.86 eV at the Fermi energy under the O-rich condition, 6.77 eV smaller than that under the O-deficient condition, while the formation energy of V_O at the Fermi energy is 4.38 eV larger by contrast. Considering the formation energy data, V_{Al}, O_{Al} and O_i (＜2.8 eV) will be readily formed in α-Al_2O_3 in an O-rich environment, while in an O-deficient environment V_{Al} and V_O will be presented. Therefore, the defect states in α-Al_2O_3 depend on the environment condition.

Interestingly, earlier studies have neglected the defects of antisite atoms O_{Al} and Al_O without giving convincible evidence [6, 22, 29]. Maybe it is thought that two steps are needed to form an antisite atom by introducing an atom into a crystal vacancy, which will consume extra energies. In fact, the formation energy of O_{Al} in α-Al_2O_3 is comparable with V_{Al}, and smaller than that of O_i in an O-rich environment, as shown in Fig.1a, giving a new insight on the defect property in α-Al_2O_3. However, the formation energies of Al_O under the O-rich condition, and both O_{Al} and Al_O under the O-deficient condition are too high to form in α-Al_2O_3 at the equilibrium state. Therefore, the defect of antisite atom O_{Al} should be considered under the O-rich condition for defect studies in α-Al_2O_3.

3.2 Schottky defect in α-Al_2O_3

The Schottky defect incorporates a few cation and anion vacancies in α-Al_2O_3, and generally is considered artificially to be of quintet, i.e. $2V_{Al}^{3-}+3V_O^{2+}$, since Al_2O_3 is an ionic compound which is consisted of Al^{3+} and O^{2-} [26, 29]. However, it should be a little questionable. Seen from Fig.1, within the whole range of Fermi level of α-Al_2O_3, the main stable charge state is 0 (V_O^{0}) for V_O, and -3 (V_{Al}^{3-}) for V_{Al}, with a little proportion of +1 and +2 charge states for V_O, and -2, -1 and 0 states for V_{Al}. Therefore, the Schottky defect in α-Al_2O_3 could have several combinations except $2V_{Al}^{3-}+3V_O^{2+}$. For this reason, we have calculated the formation energies of the following combinations of $2V_{Al}^{3-}+3V_O^{2+}$, $2V_{Al}^{1-}+V_O^{2+}$, $V_{Al}^{3-}+3V_O^{1+}$, $V_{Al}^{2-}+2V_O^{1+}$ and $V_{Al}^{q-}+V_O^{q+}$ (q=0, 1, 2) with different vacancy distances in the (2×2×2) α-Al_2O_3 supercell. The energies obtained are too large (636~1423 Ha, 1 Ha=27.211 eV), indicating that the vacancies should be separated sufficiently far from each other to form Schottky defect. An extreme condition is considered, i.e. the vacancies are infinitely separated with no interactions. If a Schottky defect forms, the formation energy of each consisting part should have an equal value. Fig.2 plots the formation energy variations of each charge state for V_{Al} and V_O within the whole Fermi level under the O-rich condition. From this figure, there are four types of possible Schottky defect, i.e. $\{V_O^{1+}:V_{Al}^{1-}\}$, $\{V_O^{2+}:V_{Al}^{2-}\}$, $\{V_O^{2+}:2V_{Al}^{1-}\}$, $\{3V_O^{2+}:2V_{Al}^{3-}\}$, and the average formation energies are 4.15 eV, 3.61 eV, 3.21 eV and 4.18 eV, respectively. According to the thermal dynamical theory, the main Schottky defect is $\{V_O^{2+}:2V_{Al}^{1-}\}$ for its smallest formation energy rather than the common considered $\{3V_O^{2+}:2V_{Al}^{3-}\}$ under the O-rich condition. On the other hand, the formation energy differences of these four types of Schottky defect are so small (＜1.0 eV) that not a single one will be absolutely dominate in α-Al_2O_3. Therefore, four types of Schottky defect will be present with different proportions ($\{V_O^{2+}:2V_{Al}^{1-}\}$ the maximum, and $\{3V_O^{2+}:2V_{Al}^{3-}\}$ the minimum) in α-Al_2O_3 under the condition of O-rich, giving a new perspective on Schottky defect in α-Al_2O_3.

Using the same approach, the case of Schottky defect under the O-deficient condition is shown in Fig.3. It can be seen that there are six types of possible Schottky defect, i.e. $\{V_O^{1+}:V_{Al}^{1-}\}$, $\{V_O^{2+}:V_{Al}^{2-}\}$, $\{V_O^{2+}:2V_{Al}^{1-}\}$, $\{2V_O^{1+}:V_{Al}^{2-}\}$, $\{3V_O^{1+}:V_{Al}^{3-}\}$, $\{3V_O^{2+}:2V_{Al}^{3-}\}$, and the average formation energies are 5.27 eV, 4.72 eV, 6.19 eV, 3.97 eV, 3.54 eV and 4.18 eV, respectively. Obviously, the main Schottky defect under the O-deficient condition is $\{3V_O^{1+}:V_{Al}^{3-}\}$ which is still out of the common consideration of $\{3V_O^{2+}:2V_{Al}^{3-}\}$. Considering the little energy differences ($<$1.0 eV) between the last three defect types, the Schottky defect of $\{2V_O^{1+}:V_{Al}^{2-}\}$, $\{3V_O^{1+}:V_{Al}^{3-}\}$ and $\{3V_O^{2+}:2V_{Al}^{3-}\}$ will be dominate in α-Al_2O_3 under the condition of O-deficient, also giving a new perspective on Schottky defect in α-Al_2O_3. By contrast with the O-rich condition, there are two more types ($\{2V_O^{1+}:V_{Al}^{2-}\}$ and $\{3V_O^{1+}:V_{Al}^{3-}\}$) of Schottky defect existing in Al_2O_3 under the O-deficient condition. For the same four defect types, the formation energies of the first two under the O-deficient condition are ~1.1 eV higher than that under the O-rich condition; while the largest energy of Schottky defect $\{V_O^{2+}:2V_{Al}^{1-}\}$ under the O-rich condition is about 3 eV higher than that in the case of O-rich, which is nearly difficult to form for its high formation energy. Interestingly, the Schottky defect $\{3V_O^{2+}:2V_{Al}^{3-}\}$ has the identical formation energy under both conditions, indicating its independence of oxygen environment, which is in good agreement with other earlier results [22, 29].

3.3 Frenkel defect in α-Al_2O_3

There are two types of Frenkel defect in α-Al_2O_3, i.e. a cation Frenkel defect $\{Al_i:V_{Al}\}$ and an anion Frenkel defect $\{O_i:V_O\}$. Generally, the two types of Frenkel defect are considered to be $\{Al_i^{3+}:V_{Al}^{3-}\}$ and $\{O_i^{2-}:V_O^{2+}\}$ in charge states [22, 26, 29]. For the same reason of the main stable charge state V_O^0 within the whole Fermi level as section 3.2, situations of Frenkel defects especially the anion Frenkel defect might be some different form the common considerations. We first calculate the relative total energies of the (2×2×2) α-Al_2O_3 supercell containing both types of Frenkel defects with different separating distances of an interstitial atom from the corresponding vacancy, and the results are shown in Fig.4. It can be seen that when the Al_i atom has a separation distance of 4NN (fourth nearest neighbor) with the vacancy V_{Al}, the formed cation Frenkel defect is most stable. So does the case of anion Frenkel defect. The situation is different from that of Schottky defects, where the consisting part locates as far as possible.

Using the same approach proposed in section 3.1, the formation energies of Frenkel defects under both the O-rich and O-deficient conditions are shown in Fig.5. It can be seen that only one type of cation Frenkel defect, i.e. $\{Al_i^{3+}:V_{Al}^{3-}\}$ forms with the average formation energy of 4.81 eV under the O-rich condition (Fig.5a). While under the O-deficient condition, there are three types of possible cation Frenkel defects, i.e. $\{Al_i^{1+}:V_{Al}^{1-}\}$, $\{Al_i^{2+}:V_{Al}^{2-}\}$ and $\{Al_i^{3+}:V_{Al}^{3-}\}$, and the average formation energies are 8.80 eV、6.42 eV and 4.81 eV (Fig.5b), respectively, giving a new perspective on Al Frenkel defect in α-Al_2O_3. Considering the big formation energy differences (over 1.5 eV) for the three defects, the Frenkel defect of $\{Al_i^{3+}:V_{Al}^{3-}\}$ will readily form in α-Al_2O_3 for its smallest formation energy under the O-deficient condition. Moreover, the defect $\{Al_i^{3+}:V_{Al}^{3-}\}$ has an equal average formation energy (4.81 eV) under both conditions, indicating that the cation Frenkel defect is independent on oxygen environment, which is in good agreement with earlier results of Al_2O_3 and other materials [22, 29].

As for the anion Frenkel defect in α-Al_2O_3 (shown in Fig.5c and 6d), two possible types of defects i.e. $\{O_i^{2+}:V_O^{2-}\}$ and $\{O_i^{1+}:V_O^{1-}\}$ will form under both O conditions, with an average formation energy of 6.41 eV and 5.85 eV, respectively, indicating the same independence of oxygen potential of anion Ftenkel defects in α-Al_2O_3. However, the main anion Frenkel defect is $\{O_i^{1+}:V_O^{1-}\}$ for its lower average formation energy, other than the common considered $\{O_i^{2+}:V_O^{2-}\}$ [22, 29]. From Fig.1, it can be seen that near the Fermi energy, the most stable charge state for V_O is V_O^0, not V_O^{2+}; while that for O_i is O_i^{2-}. Therefore, the Frenkel process in α-Al_2O_3 must have a process of charge neutralization, not a simple combination of O_i^{2+} and V_O^{2-}, which may resulting in the formation of $\{O_i^{1+}:V_O^{1-}\}$. It is noted that little formation energy difference (0.56 eV) exists for the two types of anion Frenkel defects, showing that a big proportion of $\{O_i^{2+}:V_O^{2-}\}$ may also form in α-Al_2O_3 except for $\{O_i^{1+}:V_O^{1-}\}$, giving a new perspective on O Frenkel defect in α-Al_2O_3.

3.4 Antisite pair in α-Al_2O_3

There are two types of antisite atoms i.e. O_{Al} and Al_O in α-Al_2O_3, especially under the O-rich condition, the O_{Al} atom is readily form, as shown in Fig.1. For the confine of charge neutralization, we wonder to know whether antisite pair exists in α-Al_2O_3 or not? For this reason, we calculate the relative total energies of the (2×2×2) α-Al_2O_3 supercell containing both types of antisite atoms (O_{Al} and Al_O) with different separating distances, and find that when O_{Al} and Al_O atoms are located within 1NN, the formed antisite pair is most stable. Using the same approach proposed in section 3.1, the formation energies of antisite pairs under both the O-rich and O-deficient conditions are shown in Fig.6 and Fig.7. It can be seen that three types of antisite pairs, i.e. $\{Al_O^{5+}:O_{Al}^{5-}\}$, $\{Al_O^{4+}:O_{Al}^{4-}\}$ and $\{Al_O^{3+}:O_{Al}^{3-}\}$ will possible form under the O-rich condition, with average formation energies of 13.07 eV, 10.96 eV and 9.52 eV, respectively (Fig.6). These antisite pairs have such large formation energies that they are nearly unable to form at conventional conditions. We only select $\{Al_O^{3+}:O_{Al}^{3-}\}$ as the most possible antisite pair in α-Al_2O_3 for its lowest formation energy. On the other hand, under the O-deficient condition, the most possible antisite pair is also $\{Al_O^{3+}:O_{Al}^{3-}\}$ with the same formation energy of 9.52 eV as that under the O-rich condition, though there are two more possible antisite pairs i.e. $\{Al_O^{2+}:O_{Al}^{2-}\}$ and $\{Al_O^{1+}:O_{Al}^{1-}\}$, shown in Fig.7. Considering the large formation energy of antisite pair, we assume that the defect of antisite pair is unlikely form under the conventional condition. Maybe it is of partly reason that why in other studies the antisite defect and defect pair were seldom considered.

4. Conclusions

The charge states and formation energies of intrinsic point defects as vacancies, interstitials and antisite atoms in α-Al_2O_3 have been studied based on first-principle plane-wave pseudopotential calculatuions. The results obtained can be summarized as follows:

(1) Various charge states and their variation tendencies with the Fermi level under different O conditions for individual intrinsic point defects are considered. For all defect species, the ionized states of V_{Al}^{3-}, V_O^{0}, Al_i^{3+}, O_i^{2-}, Al_O^{3+}, and O_{Al}^{3-} are found to be most stable in pure Al_2O_3. The relative stability of intrinsic point defects under the O-rich condition is $V_{Al}^{3-} > O_{Al}^{3-} > O_i^{2-} > V_O^{0} > Al_i^{3+} > Al_O^{3+}$ at the Fermi energy, while that is $V_{Al}^{3-} > V_O^{0} > O_i^{2-} > Al_i^{3+} > O_{Al}^{3-} > Al_O^{3+}$ under the O-deficient condition. From the formation energies of individual point defects, the antisite atom O_{Al} will be readily formed in α-Al_2O_3 under the O-rich condition.

(2) Four types of possible Schottky defects, i.e. $\{V_O^{1+}:V_{Al}^{1-}\}$, $\{V_O^{2+}:V_{Al}^{2-}\}$, $\{V_O^{2+}:2V_{Al}^{1-}\}$, $\{3V_O^{2+}:2V_{Al}^{3-}\}$ with the most stable species of $\{V_O^{2+}:2V_{Al}^{1-}\}$ will be formed under the O-rich condition; while six types of possible Schottky defects, i.e. $\{V_O^{1+}:V_{Al}^{1-}\}$, $\{V_O^{2+}:V_{Al}^{2-}\}$, $\{V_O^{2+}:2V_{Al}^{1-}\}$, $\{2V_O^{1+}:V_{Al}^{2-}\}$, $\{3V_O^{1+}:V_{Al}^{3-}\}$, $\{3V_O^{2+}:2V_{Al}^{3-}\}$ with the most stable species of $\{3V_O^{1+}:V_{Al}^{3-}\}$ will be formed under the O-deficient condition.

(3) Only one type of cation Frenkel defect, i.e. $\{Al_i^{3+}:V_{Al}^{3-}\}$ will be formed under the O-rich condition, while under the O-deficient condition, there will be three types of possible cation Frenkel defects, i.e. $\{Al_i^{1+}:V_{Al}^{1-}\}$, $\{Al_i^{2+}:V_{Al}^{2-}\}$ and $\{Al_i^{3+}:V_{Al}^{3-}\}$ with the most stable species of $\{Al_i^{3+}:V_{Al}^{3-}\}$. As for the anion Frenkel defect, two possible types of defects i.e. $\{O_i^{2+}:V_O^{2-}\}$ and $\{O_i^{1+}:V_O^{1-}\}$ will form under both O conditions, and the latter is the most stable for its lower formation energy.

(4) Three types of possible antisite pairs, i.e. $\{Al_O^{5+}:O_{Al}^{5-}\}$, $\{Al_O^{4+}:O_{Al}^{4-}\}$ and $\{Al_O^{3+}:O_{Al}^{3-}\}$ will be formed under the O-rich condition, and two more possible types i.e. $\{Al_O^{2+}:O_{Al}^{2-}\}$ and $\{Al_O^{1+}:O_{Al}^{1-}\}$ will be formed under the O-deficient condition. The most stable antisite pair is $\{Al_O^{3+}:O_{Al}^{3-}\}$ under both O conditions.

(5) Based on the above results, the charge states and existing forms of the intrinsic point defect processes depend on the environment conditions. Considering the most stable defect processes, the stability of defect process ranks as Schottky defect > cation Frenkel > anion Frenkel > antisite pair, indicating that the Schottky defects are dominant in pure Al_2O_3, which is consistent with experiment.

Acknowledgements

This work is supported by National Magnetic Confinement Fusion Science Program (No.2013GB110006B) and National Natural Science Foundation of China (No.21471137, No. 11275175).

Notes and references

R. H. Doremus, Alumina. In: Ceramic and Glass Materials: Structure, Properties and Processing, J. F. Shackelford and R. H. Doremus (eds.), Springer 2008, 1-26.
J. Cai, Y. Li, J. M. Wu, G. P. Ling, *Oxid. Met.*, 2014, **81**, 253.
A. H. Heuer, D. B. Hovis, J. L. Smialek, and B. Gleeson, *J. Am. Ceram. Soc.*, 2011, **94**, S146.
4 K. Shirvani, S. Mastali, A. Rashidghamat, and H. Abdollahpour, *Corros. Sci.*, 2013, **75**, 142.
J. K. Bristow, D. Tiana, S. C. Parker, and A. Walsh, *J. Mater. Chem. A*, 2014, **2**, 6198.
G. K. Zhang, Y. J. Lu, and X. L. Wang, *Phys. Chem. Chem. Phys.*, 2014, **16**, 17523.
A. H. Heuer, T. Nakagawa, M. Z. Azar, D. B. Hovis, J. L. Smialek, B. Gleeson, N. D. M. Hine, H. Guhl, H. S. Lee, P. Tangney, W. M. C. Foulkes, and M. W. Finnis, *Acta Mater.*, 2013, **61**, 6670.
C. Freysoldt, B. Grabowski, T. Hickel, and J. Neugebauer, *Rev. Mod. Phys.*, 2014, **86**, 253.
M. Choi, A. Janotti, and C. G. Van de Walle, *J. Appl. Phys.*, 2013, **113**, 044501.
Y. Kitaoka, K. Nakamura, T. Akiyama, T. Ito, M. Weinert, and A. Freeman, *Phys. Rev. B*, 2013, **87**, 205113.
S. K. Mohapatra, S. K. Tiku, and F. A. Kröger, *J. Am. Ceram. Soc.*, 1979, **62**, 50.
F. A. Kröger, *Solid State Ionics*, 1984, **12**, 189.
S. K. Mohapatra, and F. A. Kröger, *J. Am. Ceram. Soc.*, 1978, **61**, 106.
B. G. Draeger, and G. P. Summers, *Phys. Rev. B*, 1979, **19**, 1172.
G. Moya, J. Kansy, A. S. Ahmed, J. Liebault, F. Moya, and D. Goeuriot, *Phys. Stat. Sol. A*, 2003, **198**, 215.
K. P. Muthe, K. Sudarshan, P. K. Pujari, M. S. Kulkarni, N. S. Rawat, B. C. Bhatt and S. K. Gupta, *J. Phys. D: Appl. Phys.*, 2009, **42**, 105405.
S. Ikeda, and T. Uchino, *J. Phys. Chem. C*, 2014, **118**, 4346.
K. P. D. Lagerlöf, R. W. Grimes, *Acta Mater.*, 1998, **46**, 5689.
C. R. A. Catlow, R. James, W. C. Mackrodt, and R. F. Stewart, *Phys. Rev. B*, 1982, **25**, 1006.
R. W. Grimes, *J. Am. Ceram. Soc.*, 1994, **77**, 378.
G .J. Dienes, D. O. Welch, C. R. Fischer, R. D. Hatcher, O. Lazareth, and M. Samberg, *Phys. Rev. B*, 1975, **11**, 3060.
N. D. M. Hine, K. Frensch, W. M. C. Foulkes, and M. W. Finnis, *Phys. Rev. B*, 2009, **79**, 024112.
D. Liu, and J. Robertson, *Microelectron. Eng.*, 2009, **86**, 1668.
A. A. Sokol, A. Walsh, C. R. A. Catlow, *Chem. Phys. Lett.*, 2010, **492**, 44.
Y. Kumagai, and F. Oba, *Phys. Rev. B*, 2014, **89**, 195205.
N. D. M. Hine, K. Frensch, M. W. Finnis, W. M. C. Foulkes, and A. H. Heuer, *Int. Conf. on QMC*, April 6, 2009, Apuan.
A. F. Kohan, G. Ceder, D. Morgan, and Chris G. Van de Walle, *Phys. Rev. B*, 2000, **61**, 15019.
S. B. Zhang, S. H. Wei, and A. Zunger, *Phys. Rev. B*, 2001, **63**, 075205.
K. Matsunaga, T. Tanaka, T. Yamamoto, and Y. Ikuhara, *Phys. Rev. B*, 2003, **68**, 085110.
B. Delley, *J. Chem. Phys.*, 2000, **113**, 7756.
J. A. White, and D. Mbird, *Phys. Rev. B*, 1994, **50**, 4954.
B. Delley, *J. Chem. Phys.*, 1990, **92**, 508.
J. P. Perdew, K. Burke, and M. Ernzerhof, *Phys. Rev. Lett.*, 1996, **77**, 3865.
T. Kurita, K. Uchida, and A. Oshiyama, *Phys. Rev. B*, 2010, **82**, 155319.
S. B. Zhang, S. H. Wei, A. Zunger, and H. Katayama-Yoshida, *Phys. Rev. B*, 1998, **57**, 9642.
C. Kílíç, and A. Zunger, *Phys. Rev. Lett.*, 2002, **88**, 095501.
B. D. Evans, G. J. Pogatshnik, and Y. Chen, *Nucl. Instrum. Meth. B*, 1994, **91**, 258.

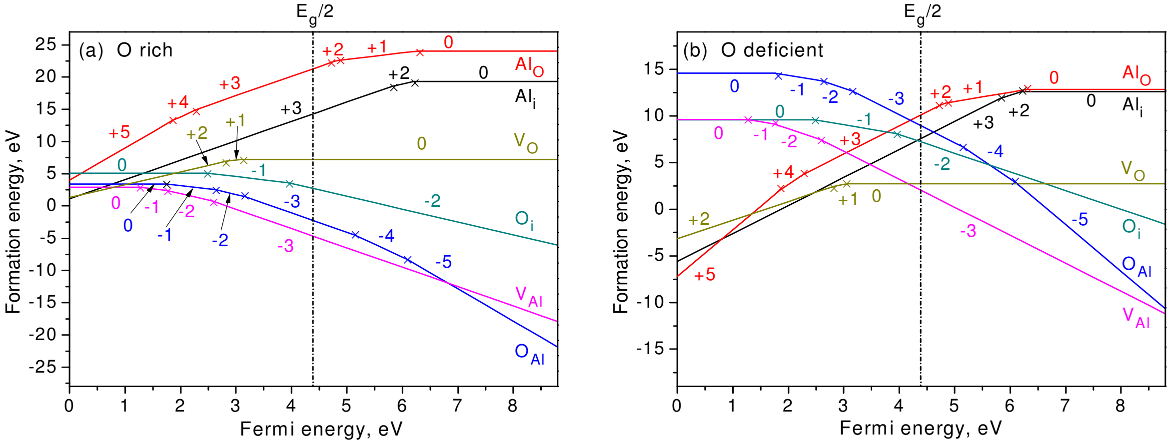

Fig.1 Formation energies of isolated intrinsic point defects in various charge states in α-Al_2O_3 as a function of the Fermi level E_F under the condition of O-rich (a) and O-deficient (b).

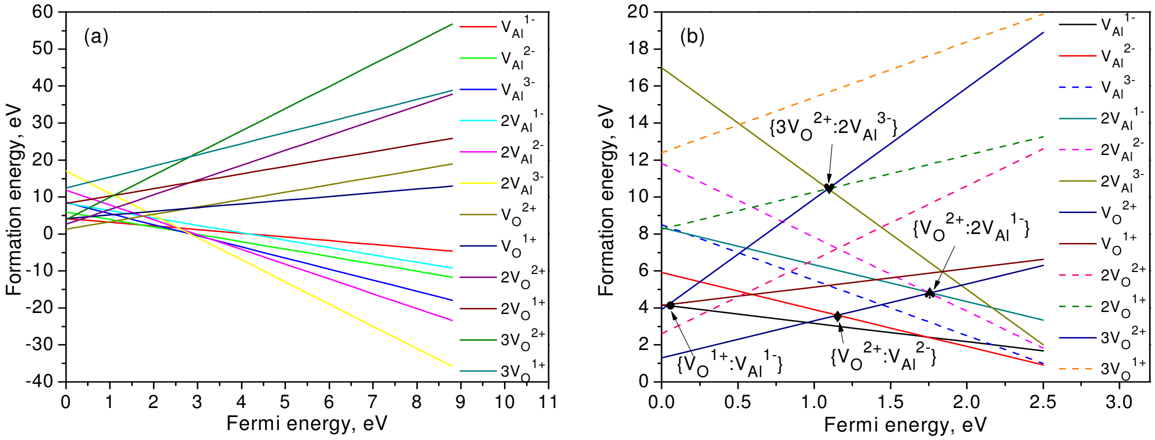

Fig.2 (a) Formation energies of several aluminum and oxygen vacancies, and (b) possible Schottky defect combinations formed in α-Al_2O_3 under the condition of O-rich.

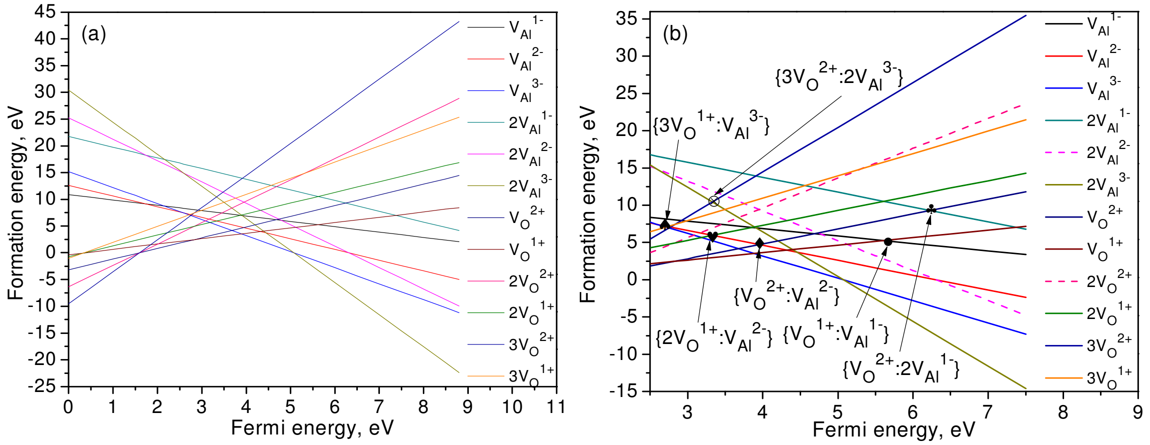

Fig.3 (a) Formation energies of several aluminum and oxygen vacancies, and (b) possible Schottky defect combinations formed in α-Al_2O_3 under the condition of O-deficient.

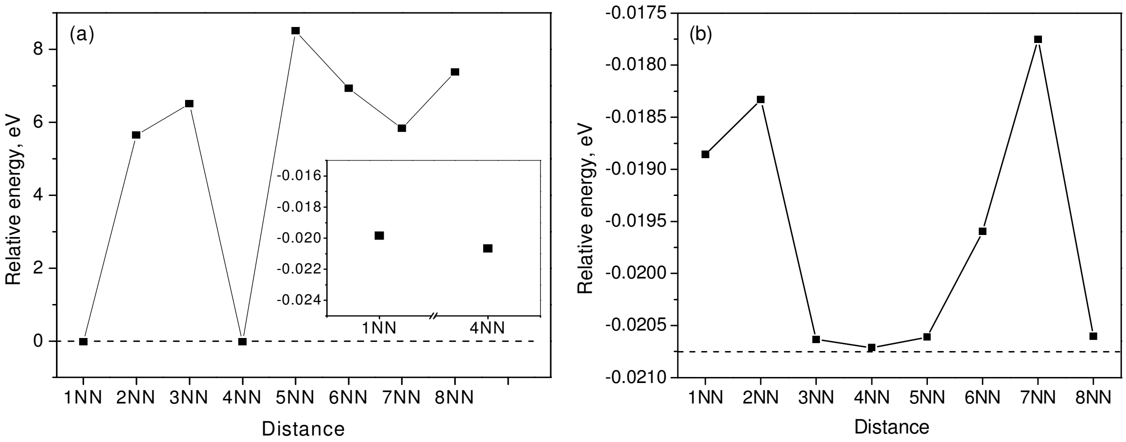

Fig.4 Relative energies of the 2×2×2 α-Al_2O_3 supercell containing a pair of (a) aluminum and (b) oxygen Frenkel defect as a function of separation distance of corresponding interstitial atom and vacancy.

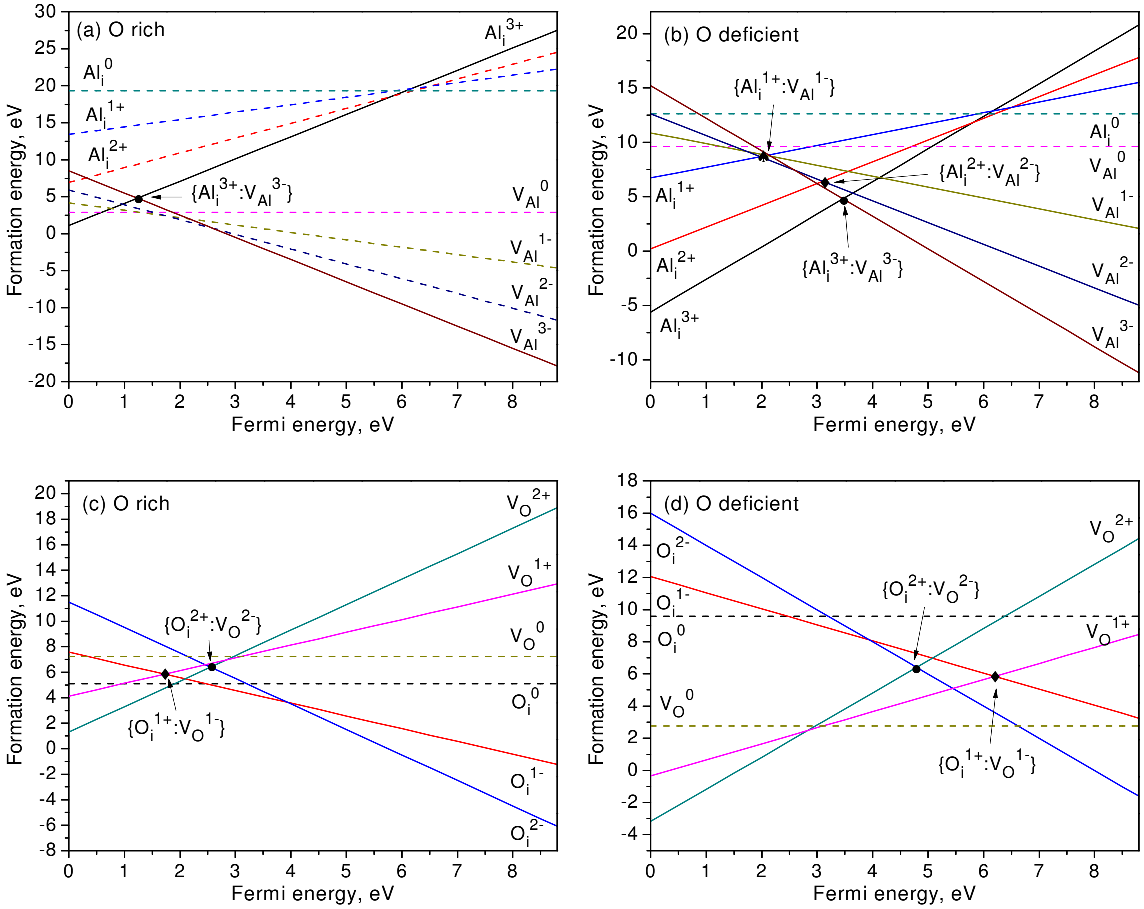

Fig.5 Possible Frenkel defect combinations formed in α-Al_2O_3 under different oxygen conditions

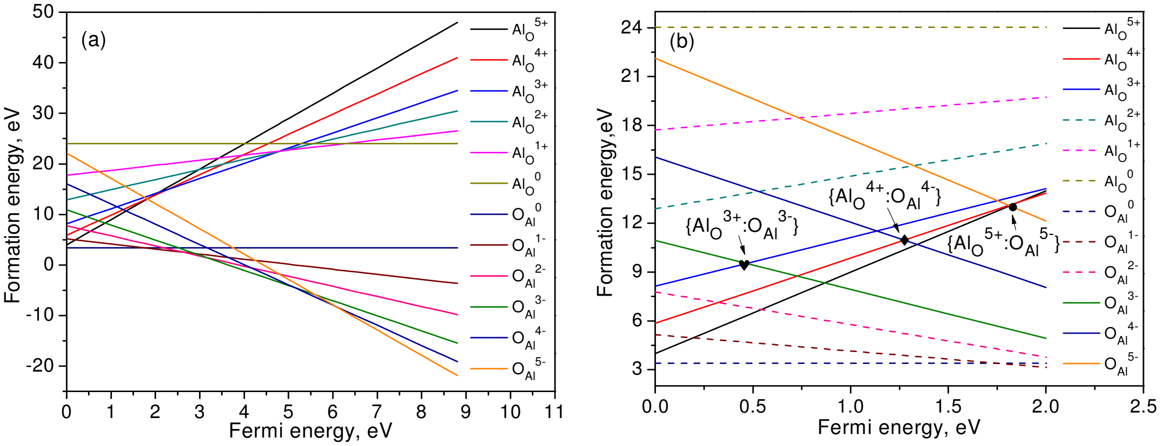

Fig.6 (a) Formation energies of antisite atom with various charge states, and (b) possible antisite defect combinations formed in α-Al_2O_3 under the condition of O-rich.

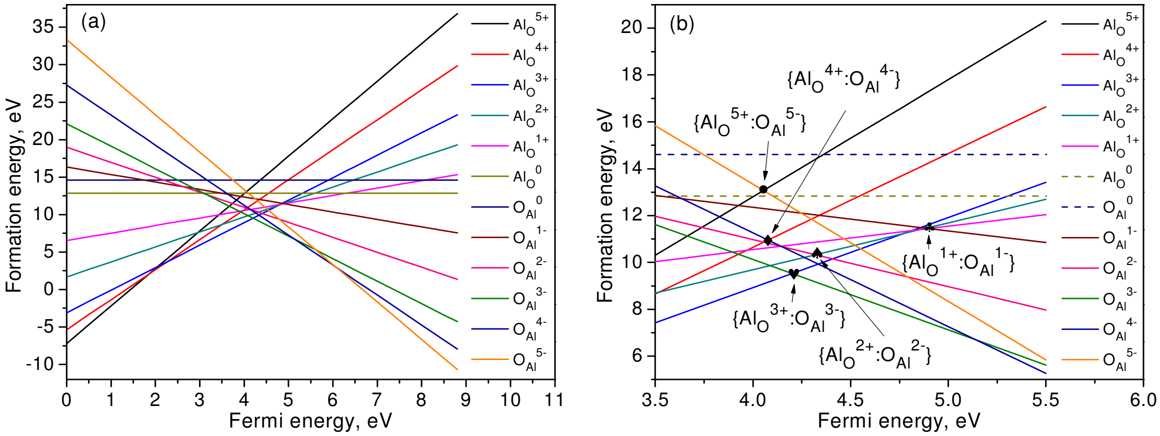

Fig.7 (a) Formation energies of antisite atoms with various charge states, and (b) possible antisite defect combinations formed in α-Al_2O_3 under the condition of O-deficient.